Heat Transfer Project Report

Solar Oven Project

Heat Transfer
MENG - 3411 - 010
Dr. Manuel Garcia

Report Group
Alan Backlund
Joseph Gomez
John Carrico

Abstract

Solar ovens are devices that offer an inexpensive way to cook, and heat foods, or sterilize water (Aalfs, 2010). The purpose of this report was to be able demonstrate design analysis processes to obtain temperatures capable of doing such, and then determine if predicting the temperature of a container filled with water using theoretical methods is possible and comparing it to the actual results of an experiment (Abhishek Saxena, 2011). Tracking the total available power input though the surface glass of the oven is analyzed in detail, while view factors and shape factors are determined to estimate the total heat losses of the oven. Optimizations to the design are then made, based on such analyses, and an oven was constructed. Using experimental data collection methods typical of such an experiment involving water temperatures, temperature predictions with respect to time from experimentation are then compared to theoretical models utilizing the lumped capacitance method. Additionally, a solar powered fan introduces principles related to Newton's Laws of cooling and changes the rate of heat transfer from the oven air to the water inside of the container. The changes in temperature over time for forced convection heating with the fan, and free convection heating with no fan are compared and discussed. Future predictions to the temperature change over time can be theoretically modeled using this method, which adds to the usefulness of the solar oven by giving the user a way to determine if the oven might be suitable for a certain use.

Introduction

Solar ovens are most often used in locations where cheap alternatives are needed to heat and cook foods and liquids and have the benefit of plenty of sunlight, and because of that have become increasingly popular.

The theoretical modeling and experimentation processes offer a new level of understanding into the heat transfer methods of radiation, convection, and conduction. The goal was to design a box oven (Abhishek Saxena, 2011) which would be tested in a location that offered plenty of sunlight using free convection and forced convection from a fan, construct theoretical models that would predict the energy coming into, and leaving the oven, then construct the oven with ideal conditions for San Angelo Texas being factored into the design. Experimentation is to then be performed under ideal conditions, and then the values gathered from these experiments would be compared to the theoretical model, based on principles learned in a heat transfer course.

Materials

- Plywood 0.75”
- Plywood 0.25”
- Polyisocyanurate foam insulation board 0.75”

- Polystyrene foam insulation board 0.75”
- Computer fan 120mm-120mm
- Solar Panel
- Window Pane
- Gorilla Heavy Duty construction adhesive
- White Lightning 3006 Advanced Formula All Purpose Caulk
- Varathane Black Classic Wood Stain
- Hillman 0.75” Flat Interior/Exterior Wood Screws

Design and Construction

The idea for the design of the oven was to create a straightforward box of simple geometry, that had a glass window large enough to gather the most possible sunlight throughout much of the day, given the amount of space taken up by the oven (Aalfs, 2010). The design was digitally constructed using SolidWorks and Google Sketchup as well as shown in the CAD rendering in Figure 1a. The glass surface will be angled to 30° in order to allow for as much average sunlight throughout the entire year to be collected and absorbed into the interior. On these days of experimentation, the front of the oven will be lifted, to bring the total angle to 15°, as explained later in this report (Abhishek Saxena, 2011).

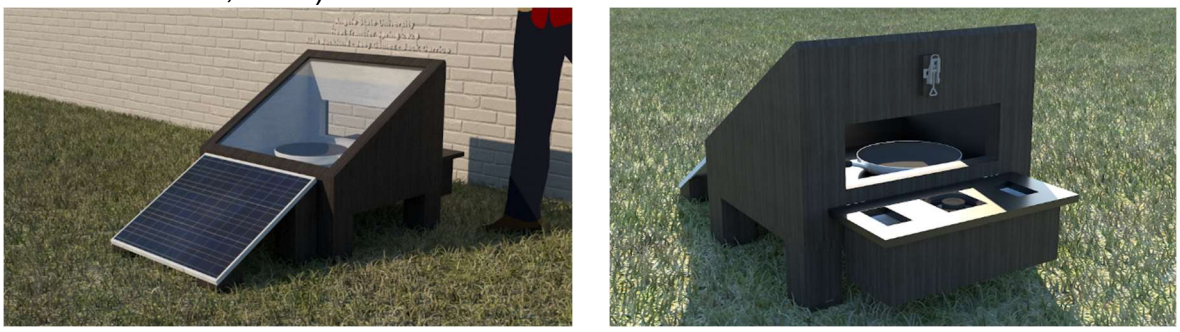

Figure 1: a) 3D SketchUp Model Front [left] b) 3D SketchUp Model Rear [right]

The solar panel’s only purpose is to power the fan, which will be used to provide forced convection, as shown in the back of the box in Figure 1b. The openings on either side of the fan will allow for air flow from the oven’s main chamber to circulate through the fan and be directed onto the can of water that will used in experimentation.

The entire inside was designed to have foam shown in the CAD image in Figure 2a and an extracted view of the foam layer in Figure 2b which would help in reducing the amount of heat loss from the oven.

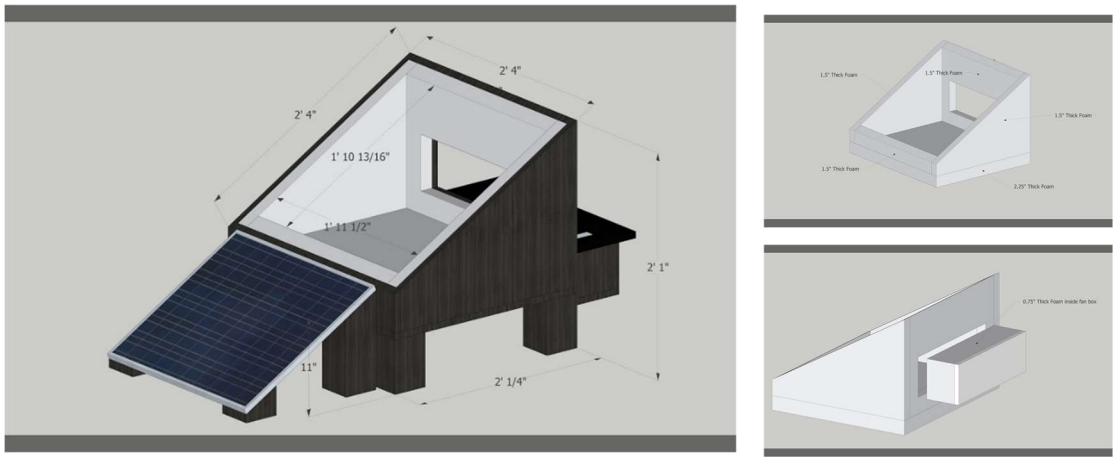

Figure 3: a) CAD Total View [left] b) CAD Insulation Front [top right] c) CAD Insulation Rear [bottom right]

The oven was constructed using .25'' plywood for the walls of the main chamber and fan compartment and as well as for the base of the oven and held together using 0.75" Flat Interior/Exterior Wood Screws. The final construction of the outer portion of

Figure 2: a) Final Solar Oven Front [left] b) Final Solar Oven Rear [right]

the oven with airflow compartment is shown in Figure 3. Once the main chamber of the oven was constructed, 0.75" Polystyrene foam insulation board was cut and placed into the interior covering the sections of the main chamber and airflow compartment. However, the initial insulation melted due to the extreme temperatures within the compartment and the damaged insulation was removed and replaced with 0.75" Polyisocyanurate foam insulation board which allowed for higher temperature resistance. Then a .25" Plywood was then installed on top of the foam for added protection as shown in Figure 4. The final step of the construction process was to install the glass and sealed with White Lightning 3006 Advanced Formula All Purpose Caulk and Gorilla Heavy Duty construction adhesive


Figure 4: a) Solar Oven with Glass [left] b) Solar Oven with Solar Panel [right]

Procedures

Theoretical

In order to compare the results in the experiment to something, it was necessary to obtain theoretical values using the analytical methods of convection, conduction and radiation. First and foremost, the amount of energy from the sun, via irradiation, is something that we must be able to measure in some way. Without sophisticated digital measuring devices to properly account for the irradiation at a given location, tabulated data can be used to estimate the amount that a given location receives.

Using the angle of elevation of the sun, relative to the horizon, and the azimuth angle as it moves from the eastern portion of the sky towards the west, a projection of a surface of interest can be calculated, which can then be used to determine the amount of heat flux from the sun is reaching that particular surface (Abhishek Saxena, 2011). For the purposes of developing a theoretical model to predict the amount of energy coming in and out of the solar, the surface areas of the glass was to be referenced as the projection surface, as this was the primary source of energy reaching the interior of the oven throughout the day (Theodor L. Bergman, 2017). According to these projections, calculated using the equation $Orthographic\ Projection\ =\ cos(\theta_{elev}) * cos(\theta_{rot}) * A_{glass}$, a maximum amount of solar energy entering the oven for each minute of the day was calculated. As seen in Figure 8, the amount of energy coming into the oven changes as the sun moves across the sky, and also, the rotation of the oven to 180° south, maximizes the amount of watts coming into the oven in the amount of 343 watts, when assuming Gs = 1000 watts/m^2. In theoretical models, we can reasonably assume that total heat losses from the oven will not exceed the heat gain from solar radiation.

In order to find the heat loss in watts leaving through the entire oven through conduction the shape factors were considered. The shape factor equations for the edges $S = 0.54 * D$, walls $S = A/L$and the corners $S = 0.15 * L$ were determined. The values determined for 4 corners was .043825, the total value of the walls was 9.9797167, and the total value of the edges was 2.0916888. Figure 6 shows a breakdown of the variables for each section of the oven. Once the shape factors for all the sections of the oven were determined and a weighted average was taken for each of the materials used in each section, then the conduction heat rate was calculated using the equation $q_{loss} = T_{s\,outside} * (2 * (.54 * D_1)^2 + 2 * (.54 * D_2)^2 + 2 * (.54 * D_3)^2 + 2 * (.54 * D_4)^2 + (A/L)_{floor} + 2 * (A/L)_{side} + (A/L)_{front} + (A/L)_{back} + 4 * (.15 * L)^4) + k_{glass} * A_{glass} * (T_{s\,inside} - T_{s\,outside})$ based off of the equation $q = kS(T_1 - T_2)$ (Theodor L. Bergman, 2017) was used to find the heat rate loss through all portions considered inside the oven chamber. Under the conditions that were present in later experiments, it was estimated

Shape Factors						
	Numbers	Thickness	Distance	Area	Shape Factor (S)	
Back/Front edg	2	0.063499966	0.482599739		.54D	0.521207719
Side edges (ver	2	0.06350	0.12700		.54D	0.137159926
Back/Front edg	2	0.07303	0.71120		.54D	0.768095585
Side edges (hor	2	0.07303	0.61595		.54D	0.665225641
Floor	1	0.08255	0.58420	0.30048	A/L	3.640022665
Side walls	2	0.10160	0.51435	0.11431	A/L	2.250285751
Front wall	1	0.06350	0.58420	0.02597	A/L	0.408940818
Back wall	1	0.06350	0.58420	0.23371	A/L	3.680467361
Corners	4	0.07303			.15L	0.043815

Figure 5: Shape Factors Data Table

that up to 87 watts of power were lost due to conduction through the walls and glass of the oven.

To find the amount of radiation leaving the oven through the glass surface, we used the view factor. To find the view factors of certain pieces in the oven, the geometry of the pieces must be explored. An equation to find the view factor is given by the double area integral $F_{12} = \frac{1}{A_1}\int_{A_1}\int_{A_2}\frac{cos\Phi_1 * cos\ ^2}{\pi * R^2}dA_1 dA_2$, which relates the two geometries to each other. An alternative method that was used in order to simplify the model. We calculated the view factors for each of the walls and the floor to the glass using the assumption that each could be approximated using the equation $F_{12} \approx 1 - sin(\theta/2)$ and then making estimations and simplifications based on the actual geometries to get a view factor number. For the front and rear walls to the glass, the geometries were what the specified equation called for. As for the sides to the glass, the view factor was assumed to be lower because the geometry did not fit the requirements exactly. The view factor of the floor to the glass was also assumed to be lower because some of the view would have been blocked due to the aluminum can. Once all of the view factors were found, they were used in the equation $q_{12} = F_{12} * J_1 * A_1$ to find the power that leaves the glass from each surface

of the oven. The surfaces of the can were left out of these equations due to the surface area being negligible relative to the interior surface area of the oven.

Experimental

Once construction had been completed pre-tests were performed to ensure thermometers were getting readings, cameras were set up to record throughout the day, and the solar oven was positioned to receive the most amount of sunlight using a solar path finder shown in Figure 5. These tests were run to determine approximately when the hottest times of the day would occur and where to place the oven to eliminate obstructions from trees. For better understanding a graphical representation of the path of the sun is shown in Figure 5c.

The actual tests were performed on 2 separate days in the afternoon in the month of May and the conditions were scattered clouds on test day 1 and clear skies on test day 2. The oven was positioned at 180° south and angled so that the face of the glass was at 15° relative to the horizon, to match the solar elevation for that day. Wind blocks were placed around the exterior of the oven to reduce the amount of heat loss due to convection on windy days (Abhishek Saxena, 2011). The unpredictable nature of wind and fluid dynamics around the oven would result in possible heat losses that are difficult to account for in calculations.

The recorded data was taken between 2:30 am and 4:15 pm with ambient air conditions between 86.11° C and 91.11 °C throughout the day the oven reached temperatures from 27.22 °C and peaking at 92.78 °C on day 1. For day 2 between the same times ambient air conditions were between 87.78 °C and 94.44 °C throughout the day where the temperature of the oven reached temperatures between 26.11 °C and 97.78 °C as shown Tables in Appendix A.

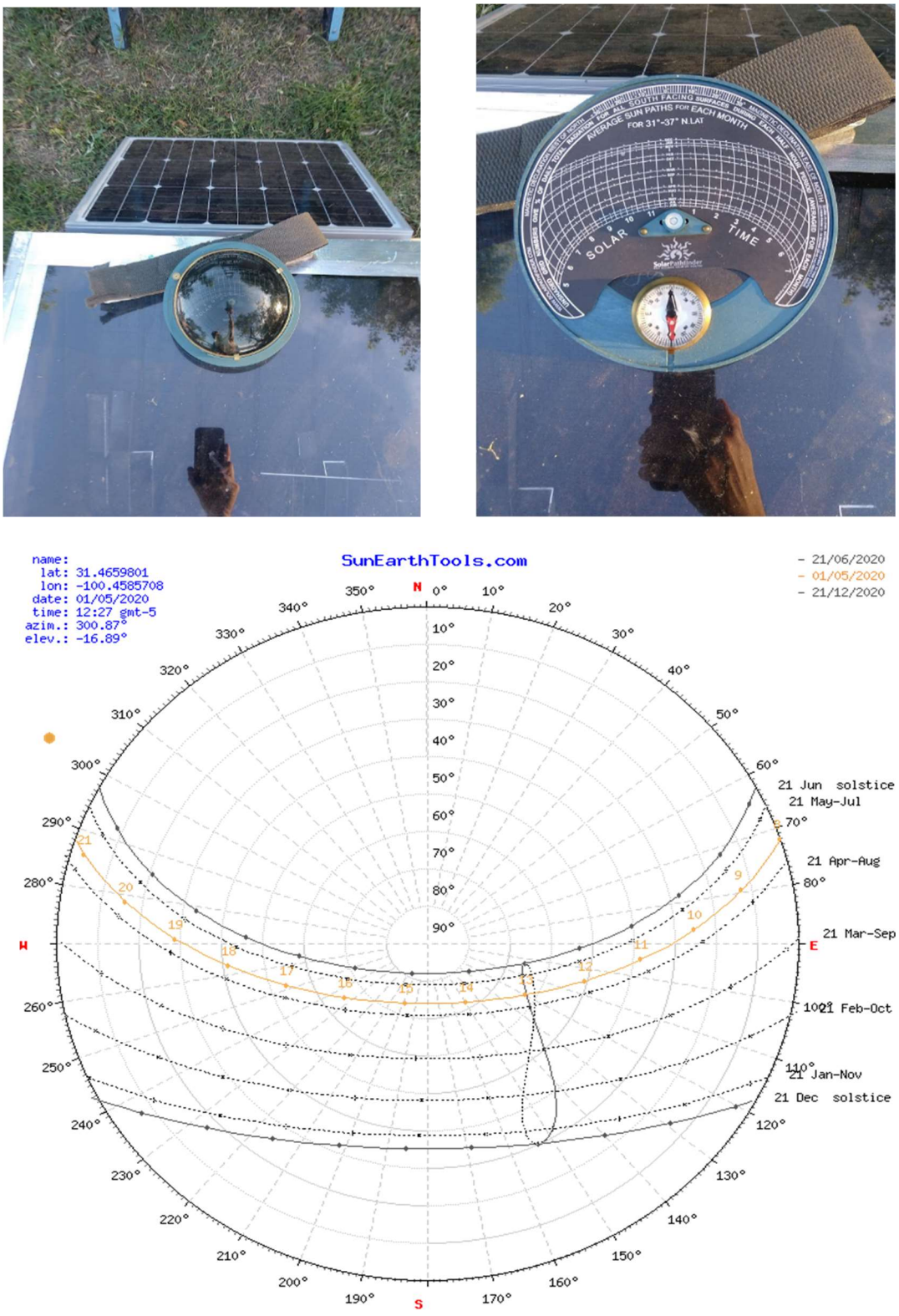

Figure 6: a) device on Solar Oven [top left] b) device Reading [top right] c) Online Representation of device [bottom]

Results and Discussion

Theoretical

As seen in Figure 7, the theoretical model with forced convection via a solar powered 120mm fan, to predict water temperature at any given point in time predicts that for 8oz of water to increase in temperature from 27.11°C to 93.32°C, it takes 75 minutes. Newton's law of cooling shows us that when forced convection across a surface occurs, a higher rate of heat transfer takes place, as compared to natural or free convection.

The theoretical model for free convection in Figure 7, shows that this is the case. The predictions made by the free convection model take into account the fluctuations in air temperature that were uncontrollable due to cloud cover that partially obstructed the view of the sun. Because the interior temperature of the oven experiences large drops in temperature when solar irradiation is reduced, a theoretical model predicts that a drop in temperature of the water will occur until the temperature of the oven increases again. This model thus predicts that for 8oz of water to increase in temperature from 27.22°C to 74.23°C, it takes 105 minutes. This can be attributed to slower rate of heat transfer from the hot internal air of the oven to the colder water that is occurring. Using the equations $\tau = \frac{\rho * \forall * c_p}{h * A_s}$, $T = e^{-t/\tau} * (T_{s\ original} - T_\infty) + T_\infty$, and $T = \frac{q_{solar}}{c_p * m} + T_\infty$, we are able to first determine a time constant τ, dependent on the density, volume, specific heat, convection coefficient, and surface area of the can, and then predict the amount of time needed to reach any temperature.

Experimental

As seen in Figure 7, the experimental results that took place on 2 consecutive days, May 1st and May 2nd of 2020, yielded results that validated the forced convection model predictions with an error up to 9% (as seen in Table 1), and did not validate the results of the free convection model as closely, with an error up to 38% (as seen in Table 2). The inconsistent temperature that was experienced in the free convection experiment within the internal airspace of the oven did not cause a noticeable drop in temperature of the water, but it is not known what reduction, if any, in the heat transfer rate occurred, as a result of this drop in temperature. The time that it took for the free convection experiment to heat 8 oz of water from 27.22°C to 76.11°C was 60 minutes, and the forced convection experiment took 75 minutes to reach 97.78°. Temperature measurements were taken every 5 minutes to account for the high rate of heat transfer, giving a higher degree of certainty with regards to the validity of the experimental results and theoretical model.

As seen in Figure 7, the experimental results and theoretical results follow similar temperature changes, with respect to time, throughout most of each experiment. Unaccounted for heat losses, or reductions in heat transfer rates are observed in the

theoretical model made to predict the temperature in the free convection experiment, but the experiment did not reflect the same decrease in temperature. These differences in the experimental results and theoretical model may be attributed to the stored heat that is present in the oven due to the mass of the plywood, foam, and glass (Aalfs, 2010). This heat storage provides a residual source of heat going into the water and helps to stabilize the temperature.

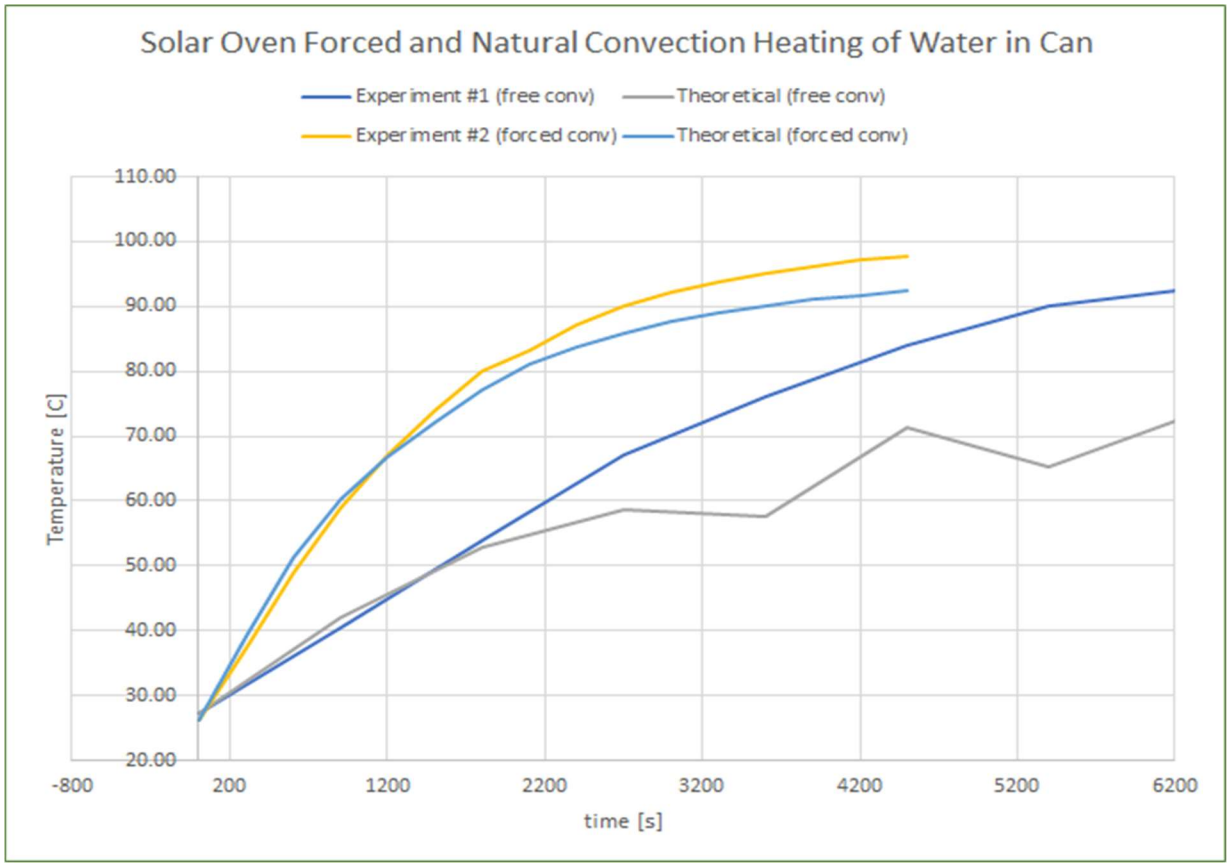

Figure 7: Solar Oven Forced and Natural Convection Heating of Water in Can

Additional improvements to the experiment could be made by increasing the amount of water in the container, thus increasing the length of time that it takes to heat it, but also extends the time that the experiment must be performed, introducing higher risks of having weather conditions change. Theoretical modeling becomes more unpredictable with time, so if the model is incorrect, the long experiment would make it very apparent that such a model was not accurate. Short experiments, for example if we only looked at a 15-minute window of time, would yield theoretical predictions with extremely low errors, but makes it difficult to trust the data.

Long experimental run times also limit the window of time during the day that an experiment can be run, due to the low elevation of the sun in the morning and evening hours. As previously discussed, the solar irradiation increases steadily throughout the day until peaking, in this case at 2:45pm, and then begins decreasing. As seen in Figure

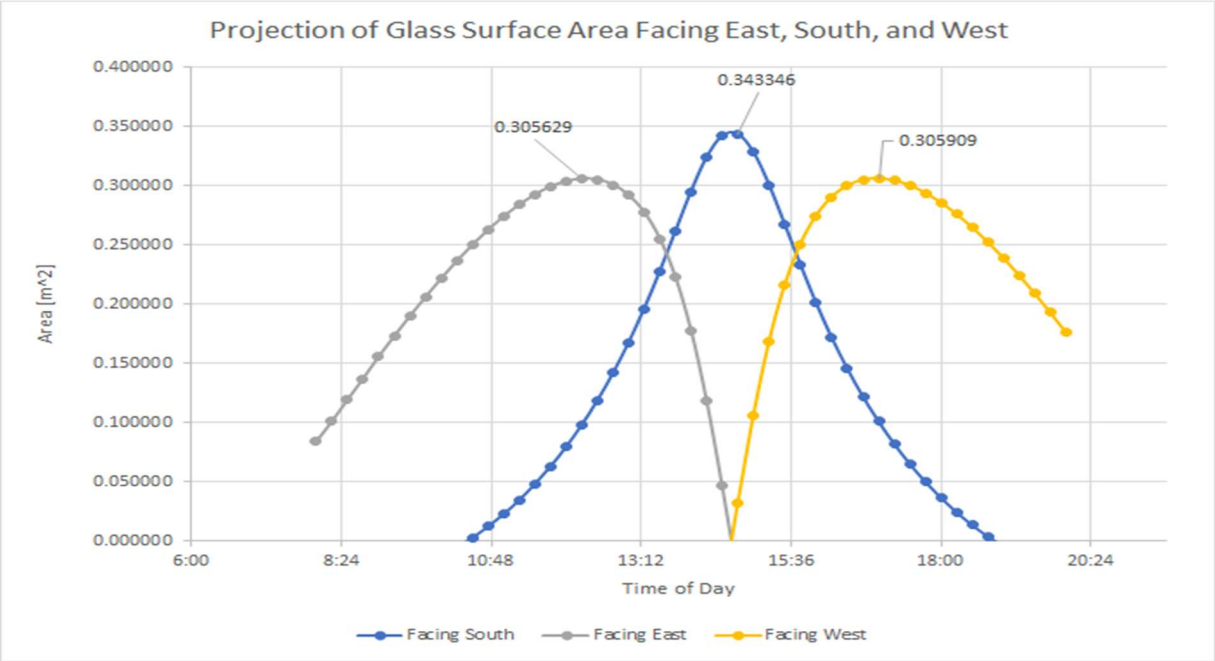

Figure 8: Projection of Glass Surface Area Facing East, South, and West

8, if the oven were faced directly east (90°), then the early hours of the day would introduce more solar energy into the top surface area of the glass, in the amount of 305.6watts (Area of 0.3056m^2 * 1000w/m^2 solar irradiation), but is a lower amount of power compared to facing the oven south. The peak power coming into the glass when the oven is turned towards the south at 180° is 343.3 watts, and 305.9 watts when faced west. As seen in these representations of the total solar energy available to the oven during any given day, rotating the oven steady at regular intervals throughout the day, could increase the total available solar irradiation to the oven throughout the day, lengthening the time available to run experiments. If this were to be studied in this report, an integral of these curves could be taken to determine the total energy input into the oven.

In order to achieve predictable temperatures, it could be beneficial to experiment only at times where the solar oven has reached steady state conditions, and the temperature inside of the oven remains constant, or close to a constant temperature rather than times when temperatures are rising or falling at fast rates.

Conclusion

In conclusion, the oven's design allows for an appropriate level of solar radiation to enter into the box, with adequate insulation amounts, and low heat loss due to air leakage, to heat water via forced or free convection, to near boiling temperatures on these particular days of experimentation in San Angelo, TX (Aalfs, 2010). With more intense solar irradiation levels nearing the summer solstice, where the sun's elevation and azimuth angle are at their max, it can be reasonably assumed that the

temperatures inside of the box will increase and the heat rates into a can of water for each theoretical and experimental models, will increase as well.

The solar oven effectively converts the sun's radiation energy into heat when entering the glass and absorbing into the black surfaces and can efficiently heat up foods or sterilize water with no additional methods of energy input into the system, other than the sun. In the cases where forced convection is desired, a fan can be powered via battery, or solar power, thus increasing the rate at which food is heated up or water is sterilized, but free convection, void of any electrical components, will sufficiently achieve the stated results as well, but at slower rates.

Improvements upon the design and construction of the box, such as a reduction in the volume of air to be heated, while maintaining a high amount of collected solar irradiation, would result in less heat losses through the surfaces of the oven (according to the laws of conduction), and higher overall air temperatures inside of the box. These improvements could help the solar oven to reach temperature ranges that would allow for safe cooking of meat, at temperatures where parasites and other harmful organisms will be killed off, to allow for sustainable cooking for people that do not have access to traditional cooking methods.

Appendix A: Raw Data

Table 1: Experimental and Theoretical Forced Convection Water Warming				
Date	**Time [s]**	**Experimental Temp. [C]**	**Theoretical Temp. [C]**	**Error %**
5/2/2020 14:30	0	26.11	26.11	0.00%
5/2/2020 14:35	300	37.22	41.31	-9.90%
5/2/2020 14:40	600	48.89	51.25	-4.62%
5/2/2020 14:45	900	58.89	60.33	-2.39%
5/2/2020 14:50	1200	67.22	66.93	0.44%
5/2/2020 14:55	1500	73.89	72.21	2.32%
5/2/2020 15:00	1800	80.00	77.13	3.71%
5/2/2020 15:05	2100	83.33	81.04	2.82%
5/2/2020 15:10	2400	87.22	83.73	4.17%
5/2/2020 15:15	2700	90.00	85.94	4.72%
5/2/2020 15:20	3000	92.22	87.70	5.16%
5/2/2020 15:25	3300	93.89	89.09	5.38%
5/2/2020 15:30	3600	95.00	90.20	5.32%
5/2/2020 15:35	3900	96.11	91.08	5.53%
5/2/2020 15:40	4200	97.22	91.77	5.94%
5/2/2020 15:45	4500	97.78	92.33	5.91%

Table 2: Experimental and Theoretical Free Convection Water Warming				
Date	**Time [s]**	**Experimental Temp [C]**	**Theoretical Temp [C]**	**Error %**
5/1/2020 14:30	0	27.22	27.22	0.00%
5/1/2020 14:45	900	40.56	41.96	-3.35%
5/1/2020 15:00	1800	53.89	52.88	1.91%
5/1/2020 15:15	2700	67.22	58.67	14.57%
5/1/2020 15:30	3600	76.11	57.61	32.12%
5/1/2020 15:45	4500	83.89	71.23	17.78%
5/1/2020 16:00	5400	90	65.22	38.00%
5/1/2020 16:15	6300	92.78	73.24	26.67%

Table 3: Constants					
Density (kg/m^3)	**Volume (m^3)**	**Cp (J/K)**	**h (W/m*K)**	**Can Surface Area (m^2)**	**Theoretical Tau**
1000	0.00024	4200	7	0.034438924	4181.315297
Density (kg/m^3)	**Volume (m^3)**	**Cp (J/K)**	**h (W/m*K)**	**Can Surface Area (m^2)**	**Theoretical Tau**
1000	0.00024	4200	22.59213562	0.034438924	1295.548485

Date:	May 1 2020										
coordin	31.4659939, -										
location	31.46599390,-										
hour	Elevation	Azimuth	hour	Elevati	Azimuth	hour	Elevation	Azimuth	hour	Elevatio	Azimuth
7:56:12	-0.833	71.43	11:15:00	41	96.94	14:30:00	73.79	172.32	17:45:00	44.79	260.33
8:15:00	2.99	73.86	11:30:00	44.17	99.32	14:45:00	73.86	185.32	18:00:00	41.62	262.73
8:30:00	6.08	75.75	11:45:00	47.32	101.87	15:00:00	73.22	197.91	18:15:00	38.44	264.98
8:45:00	9.19	77.61	12:00:00	50.43	104.67	15:15:00	71.94	209.22	18:30:00	35.26	267.11
9:00:00	12.33	79.44	12:15:00	53.5	107.76	15:30:00	70.15	218.91	18:45:00	32.06	269.14
9:15:00	15.48	81.26	12:30:00	56.52	111.24	15:45:00	67.96	226.99	19:00:00	28.86	271.1
9:30:00	18.65	83.08	12:45:00	59.46	115.22	16:00:00	65.5	233.71	19:15:00	25.67	273
9:45:00	21.84	84.92	13:00:00	62.3	119.82	16:15:00	62.83	239.32	19:30:00	22.48	274.86
10:00:00	25.03	86.77	13:15:00	65	125.25	16:30:00	60.02	244.07	19:45:00	19.3	276.7
10:15:00	28.23	88.66	13:30:00	67.51	131.73	16:45:00	57.1	248.15	20:00:00	16.13	278.53
10:30:00	31.43	90.6	13:45:00	69.75	139.54	17:00:00	54.09	251.71	20:15:00	12.97	280.35
10:45:00	34.63	92.62	14:00:00	71.63	148.9	17:15:00	51.03	254.88	20:30:00	9.84	282.19
11:00:00	37.82	94.72	14:15:00	73.02	159.92	17:30:00	47.92	257.73	20:45:00	6.72	284.04

Figure 9: Elevation and Azimuth

Appendix B: Sample Equations and Constants

Shape Factor Equations

$$Shape\ Factor\ for\ a\ Corner = 0.15 * L$$

$$Shape\ Factor\ for\ an\ Edge\ = 0.54 * D$$

$$Shape\ Factor\ for\ a\ Plane\ = A/L$$

$$q_{loss} = T_{s\ outside} * (2 * (.54 * D_1)^2 + 2 * (.54 * D_2)^2 + 2 * (.54 * D_3)^2 + 2 * (.54 * D_4)^2 + (A/L)_{floor} + 2 * (A/L)_{side} + (A/L)_{front} + (A/L)_{back} + 4 * (.15 * L)^4) + k_{glass} * A_{glass} * (T_{s\ inside} - T_{s\ outside})$$

Solar Projection Equations

$$\theta_{elev} = \theta_{fixed\ tilt} - \theta_{solar\ elev}$$

$$\theta_{rot} = |\theta_{rotation\ from\ North} - \theta_{solar\ azimuth}|$$

$$Orthographic\ Projection\ = cos(\theta_{elev}) * cos(\theta_{rot}) * A_{glass}$$

Resistance Equations

$$Conduction\ Resistance = \frac{L}{k * A}$$

$$Convection\ Resistance = \frac{1}{h * A}$$

View Factor Equations

$$F_{12} \approx 1 - sin(\theta/2)$$

$$q_{12} = F_{12} * J_1 * A_1$$

$$F_{12} = \frac{1}{A_1}\int_{A_1}\int_{A_2} \frac{cos\Phi_1 * cos\Phi_2}{\pi * R^2} dA_1 dA_2$$

Radiation Equations

$$E = \varepsilon * \sigma * {T_s}^4$$

$$J = E + (1 - \alpha) * G$$

$$q"_{rad} = J - G = E - \alpha * G$$

$$q"_{rad} = \varepsilon * \sigma * ({T_s}^4 - {T_{sur}}^4)$$

$$q_{rad}\ through\ glass = G * Orthographic\ Projection$$

$$T_{s\ outside} = \frac{\alpha * G}{h} + T_\infty$$

$$T_{s\ inside} = (\frac{q_{rad}\ through\ glass}{\sigma} + {T_{sur}}^4)^{1/4}$$

$$q"_{rad+conv} = h * (T_s - T_\infty) + h * (T_s - T_{sur})$$

Convection Equations

$$q" = h(T_s - T_\infty)$$

Lumped Capacitance Equations

$$\tau = \frac{\rho * \forall * c_p}{h * A_s}$$

$$T = e^{-t/\tau} * (T_{s\ original} - T_\infty) + T_\infty$$

$$T = \frac{q_{solar}}{c_p * m} + T_\infty$$

Percent Error Equation

$$\%\ Error = \frac{Experimental\ -\ Theoretical}{Theoretical} * 100$$

Table 4: Constants	
Absorptivity of Stained Wood (α)	0.83
Stefan-Boltzmann (σ)	5.67*10^-8
Emissivity of Stained Wood (ε)	0.85
Irradiation (G)	1000
h (free convection)	4.5
h (forced convection of fan)	22.5921
h (forced convection of wind)	23
Velocity from fan	2

Table 5: k Values		
77°F	Air	0.0262
257°F	Air	0.0333
437°F	Air	0.0398
77°F	Polystyrene/Polyiso	0.03
77°F	Plywood	0.13
77°F	Glass, window	0.96
	Floor Avg	0.0395
	Wall Avg	0.07

References

Bergman, Theodore L. Lavine, Adrienne S. “Fundamentals of Heat and Mass Transfer.” Wiley. 2017. Print.

National Weather Service. “Weather observations for the past three days. San Angelo Mathis Field.” 2020. Web. weather.gov.

“Tools for consumers and designers of solar.” 2009. Web. sunearthtools.com.

“How to calculate the temperature rise in a sealed enclosure.” 2020. Web. heatsinkcalculator.com.

Aalfs, Mark. “Principles of Solar Box Cooker Design.” The Solar Cooking Archive. 2010. Print.

Saxena, Abhishek. Varun. Pandey, S.P. Srivastav, G. “A thermodynamic review on solar box type cookers.” Elsevier. 2011. Print.